# SOME ESTIMATES OF THE POWER SPECTRA OF LARGE-SCALE DISTURBANCES IN LOW LATITUDES

*Stanley L. Rosenthal*

Los Alamos Scientific Laboratory[1]

(Manuscript received 7 August 1959)

## ABSTRACT

Power spectra, covering a range of periods of from 1.2 to 30 days, of the zonal- and meridional-wind components at the 5000- and 40,000-ft levels at seven low latitude stations are presented. A brief discussion of the spectra is given.

## 1. Introduction

In recent years, an increasing amount of attention has been devoted to the study of spectra of large-scale meteorological disturbances. To the author's knowledge, however, all published material along these lines has been restricted to extratropical and subtropical latitudes. It is the purpose of this paper to give the results of a pilot study of spectra of large-scale disturbances in low latitudes. These spectra must, however, be considered as crude and tentative. A future study is planned which will be based on larger data samples and more refined methods of calculation.

The observational material consists of tabulated upper-wind reports taken in the tropical regions of the North Pacific Ocean during Operation Redwing and published by Joint Task Force Seven [1]. For the stations considered (see table 1), upper winds are available at 6-hr intervals during the period 15 April 1956 through 23 July 1956. Thus, there are 100 days and approximately 400 observations available for each of the seven stations. The samples are by no means extensive. Additional computations with independent and larger samples are needed to check and extend our results. Furthermore, the data are geographically limited to that portion of the tropical Pacific Ocean included in the Marshall Island proving ground network. Extension of this work should then also consider stations in other tropical regions.

We have computed spectra for the zonal- and meridional-wind components at the 5000- and 40,000-ft levels. The 5000-ft level was selected because it is representative of the trade wind or easterly flow of the lower troposphere [3]. The 40,000-ft level is, on the other hand, the altitude at which the disturbances of the upper tropical troposphere reach their greatest intensity [4].

## 2. Method

If the mean-resultant wind over some period of time at a particular location is defined to be the basic current for the period and location, then it is easy to show that the sum of the variances of the zonal- and meridional-wind components is equal to twice the mean-disturbance kinetic energy per unit mass. Since a plot of the power spectrum of a time series shows the variance contributed by oscillations with various frequencies to the variance of the time series as a whole [2], the power spectra of the zonal- and meridional-wind components will then show the proportion of specific mean-perturbation kinetic energy produced by disturbances of various frequencies (or periods) in each of the wind components.

Although the theory of spectral analysis is now summarized in many places (see, for instance, Kahn [5]), we will briefly review those matters which are of significance to the present paper. The development is given for the zonal ($u$) component of the wind; the

TABLE 1. Station locations and wind statistics.

| Station | Lat. | Long. | 5000 ft<br>$\bar{u}$ (m/sec) | $\sigma_u^2$ (m/sec)$^2$ | $\bar{v}$ (m/sec) | $\sigma_v^2$ (m/sec)$^2$ | 40,000 ft<br>$\bar{u}$ (m/sec) | $\sigma_u^2$ (m/sec)$^2$ | $\bar{v}$ (m/sec) | $\sigma_v^2$ (m/sec)$^2$ |
|---|---|---|---|---|---|---|---|---|---|---|
| Tarawa | 1.4N | 172.9E | −7.6 | 17.03 | 1.1 | 5.76 | 4.5 | 80.2 | −2.6 | 28.64 |
| Kapingamarangi | 1.0N | 154.8E | −4.4 | 11.55 | 0.8 | 4.98 | 0.0 | 42.33 | −0.2 | 24.06 |
| Kusaie | 5.3N | 163.0E | −6.0 | 20.70 | 2.2 | 8.81 | 3.1 | 54.19 | −0.1 | 24.67 |
| Eniwetok | 11.3N | 162.3E | −8.8 | 13.61 | 0.9 | 6.75 | 9.9 | 111.35 | 2.5 | 61.75 |
| Guam | 13.6N | 144.9E | −8.5 | 15.14 | 0.3 | 6.54 | 3.2 | 121.31 | −1.7 | 83.68 |
| Wake | 19.3N | 166.6E | −7.1 | 11.79 | 0.7 | 5.18 | 10.8 | 197.22 | −1.8 | 157.42 |
| Marcus | 24.3N | 153.0E | −1.8 | 28.64 | 2.4 | 19.37 | −1.2 | 154.49 | −7.4 | 111.44 |

---

[1] Present affiliation: Florida State University.

development for the meridional ($v$) component is, of course, exactly the same.

Suppose we have a record of observations covering a time interval $2T$. Upon setting the origin of our time scale at the center of this interval, we may write

$$\bar{u} = \frac{1}{2T}\int_{-T}^{T} u(t)dt, \qquad (1)$$

$$u'(t) = u(t) - \bar{u}, \qquad (2)$$

$$\sigma_u^2 = \frac{1}{2T}\int_{-T}^{T} (u'(t))^2 dt. \qquad (3)$$

The usual procedure is to set $u(t) = 0$ outside the interval of observation [5; 6]. If this is done, the limits of integration in (1) and (3) may be replaced by $\pm\infty$. If $u'(t)$ satisfies the Dirichlet conditions, we may express it as a Fourier integral in the following form:

$$u'(t) = \int_{-\infty}^{\infty} U(\omega)e^{i\omega t}d\omega \qquad (4)$$

where

$$U(\omega) = \frac{1}{2\pi}\int_{-\infty}^{\infty} u'(t)e^{-i\omega t}dt; \qquad (5)$$

$i = (-1)^{\frac{1}{2}}$ and $\omega$ is the angular frequency. Now, with the aid of the Faltung Theorem, (3) may be written as

$$\sigma_u^2 = \int_{-\infty}^{\infty} \frac{U(\omega)\hat{U}(\omega)}{2T}d\omega \equiv \int_{-\infty}^{\infty} \Phi(\omega)d\omega, \qquad (6)$$

where the cirumflex indicates a complex conjugate. $\Phi(\omega)$ is, of course, a real function. Now, the imaginary part of the right side of (4) must vanish because $u'(t)$ is real. This implies that $U(\omega)$ is an even function, so we may write (6) as

$$\sigma_u^2 = \int_{0}^{\infty} 2\Phi(\omega)d\omega. \qquad (7)$$

The function $2\Phi(\omega)$ is the power spectrum of the variable (in this case, $u'(t)$). From (7), it is clear that the area enclosed by the curve $2\Phi(\omega)$ and the lines $\omega = \omega_1$, $\omega = \omega_1 + d\omega$ (when $2\Phi(\omega)$ is plotted against $\omega$) represents the contribution to the total variance of $u(t)$ produced by oscillations with angular frequencies in the range $\omega_1$ to $\omega_1 + d\omega$.

There are many methods available for evaluating $2\Phi(\omega)$ from observed data (for a summary of some of these, see Kahn [5]). The method we have used here is among those discussed by Kahn and, as he notes, it gives only crude estimates of the spectral function. The method does, however, have the attribute that if one stretches the data to compute $2\Phi(\omega)$ for relatively low frequency (long period) oscillations, this in no way influences the computed values of $2\Phi(\omega)$ at the shorter periods. This is not the case, for instance, with the more conventional method of taking the Fourier transform of the auto-correlation function.

It can be shown [5] that

$$E(r) = \int_{0}^{\infty} 2\Phi(\omega)\left[\frac{\sin\ (\omega r/2)}{\omega r/2}\right]^2 d\omega, \qquad (8)$$

where $E(r)$ is the variance of moving averages of $u(t)$ taken over time increments of duration $r$. Kahn [5] investigates the function

$$\left[\frac{\sin\ (\omega r/2)}{\omega r/2}\right]^2$$

and shows that, roughly, it can be treated as having values of 1 when $\omega \leq (\pi/r)$ and zero when $\omega > (\pi/r)$. Hence, (8) can be written as

$$E(r) \approx \int_{0}^{\pi/r} 2\Phi(\omega)d\omega. \qquad (9)$$

If $E(r)$ has been computed for two values of $r$, $r_{i+1}$ and $r_i$ $(r_{i+1} > r_i)$, we may write

$$E(r_{i+1}) - E(r_i) \approx [2\Phi(\omega)]_{i,i+1} \times \pi\left(\frac{1}{r_{i+1}} - \frac{1}{r_i}\right), \qquad (10)$$

where $[2\Phi(\omega)]_{i,i+1}$ represents the average value of $2\Phi(\omega)$ over the interval $(\pi/r_{i+1}) \leq \omega \leq (\pi/r_i)$. The corresponding angular frequency is

$$[\omega]_{i,i+1} = \frac{\pi}{2}\left[\frac{1}{r_i} + \frac{1}{r_{i+1}}\right]. \qquad (11)$$

Rearrangement of (10) yields

$$[2\Phi(\omega)]_{i,i+1} \approx \frac{r_i r_{i+1}}{\pi}[E(r_i) - E(r_{i+1})][r_{i+1} - r_i]^{-1}. \qquad (12)$$

In our computations, we have used observations at quarter-day intervals, and $E(r)$ was computed for running means of from 2 to 60 observations. Thus, if we measure time in units of days, we may write

$$r_i = i/4, \quad i = 2, 3, 4, \cdots, 60. \qquad (13)$$

When (13) is introduced into (11) and (12), we obtain our computing formulae

$$[\omega]_{i,i+1} = \frac{2\pi(2i + 1)}{i(i + 1)}, \qquad (14)$$

$$[2\Phi(\omega)]_{i,i+1} \approx \frac{i(i + 1)}{4\pi}[E(i) - E(i + 1)]. \qquad (15)$$

Equation (7) shows that if one wishes to plot the spectrum on a logarithmic scale of $\omega$, then, to preserve the property of area being proportional to variance, one must first multiply $2\Phi(\omega)$ by $\omega$. This has been done in the figures presented in the next section.

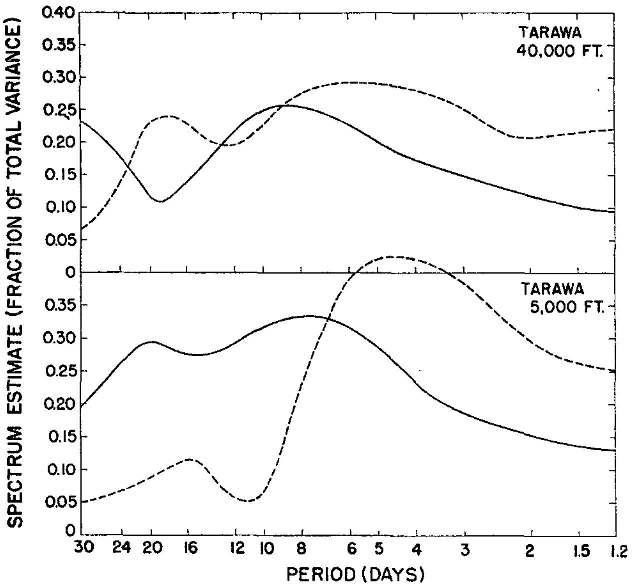

FIG. 1. Power spectra for Tarawa. Dashed lines are for $v$-component; solid lines indicate $u$-component.

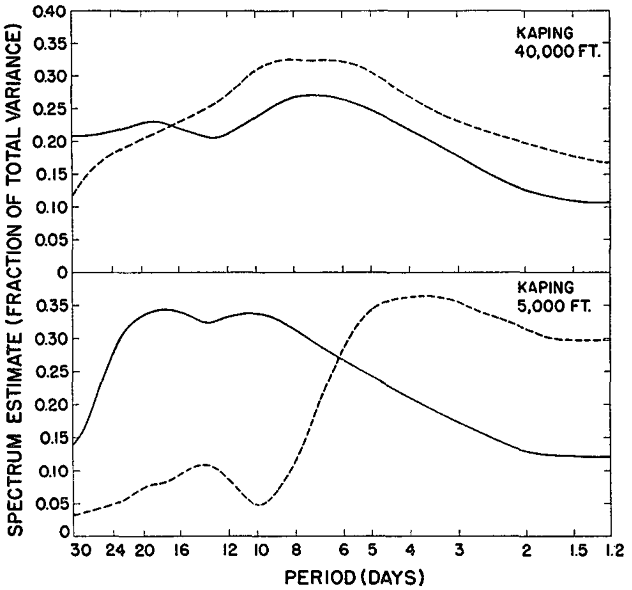

FIG. 2. Same as fig. 1 but for Kapingamarangi.

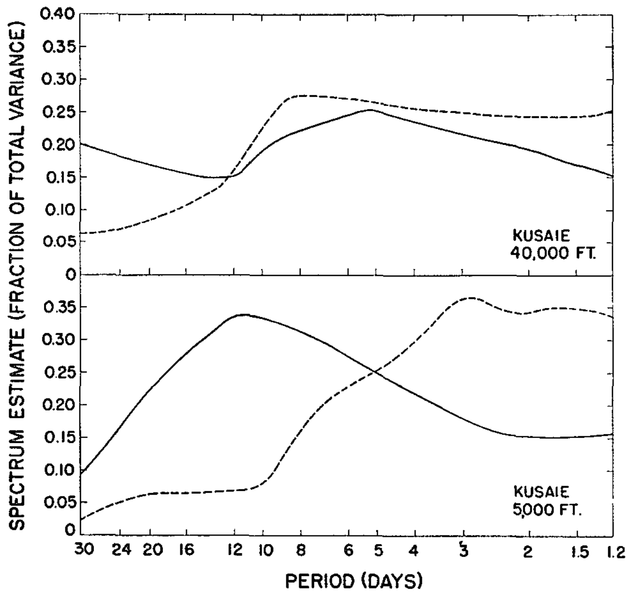

FIG. 3. Same as fig. 1 but for Kusaie.

According to Kahn [5], the degree of approximation of (9), for simple cases where the spectrum has a single maximum, is good near the maximum, high at longer periods, and low at shorter periods. This should be kept in mind during the discussion of the next section.

## 3. Results

Since we are here primarily interested in the shapes of spectra, the spectral estimates plotted on figs. 1 through 7 have been normalized through division by the variance. Hence, the areas under the spectral curves, in particular frequency bands, are proportional to fraction of total variance rather than to variance itself. Multiplication of the ordinate scale by the proper variance (table 1) will remove the normalization.

In figs. 1 through 7, the solid lines represent the spectra for the zonal-wind components; the dashed lines represent the spectra of the meridional-wind component. The lower half of each figure gives the picture for the 5000-ft level, while the upper half illustrates the situation at 40,000 ft. The curves were originally plotted on a logarithmic scale of angular frequency. However, the scale has been relabeled in terms of period. Data points have not been reproduced. For practical purposes, the reader may assume that the curves pass through all data points.

*Five-thousand feet.* With the exception of Marcus Island (fig. 7), the $v$-spectra indicate relatively large proportions of specific energy in the shorter-period oscillations and lesser amounts of energy in the longer-period oscillations. At Kapingamarangi (fig. 2) and Tarawa (fig. 1), the $v$-spectra reach distinct maxima in the vicinity of 4-day periods and drop off rapidly to minima near 10 days. The maxima at 4-days are, no doubt, a result of the passage of equatorial waves of the type discussed by Palmer [7]. At Kusaie (fig. 3), which is some four degrees north of Kapingamarangi and Tarawa, there is only a slight tendency for a peak of the $v$-spectrum and the peaking occurs in the vicinity of 3-days. At Eniwetok (fig. 4), peaking is also slight and occurs at a period of between 2 and 3 days. At the other stations, there are no maxima in the $v$-spectra at or near 4 days. This is consistent with the well known rapid poleward damping of equatorial waves in the region under discussion [7].

At Guam (fig. 5) and Wake (fig. 6), the $v$-spectra

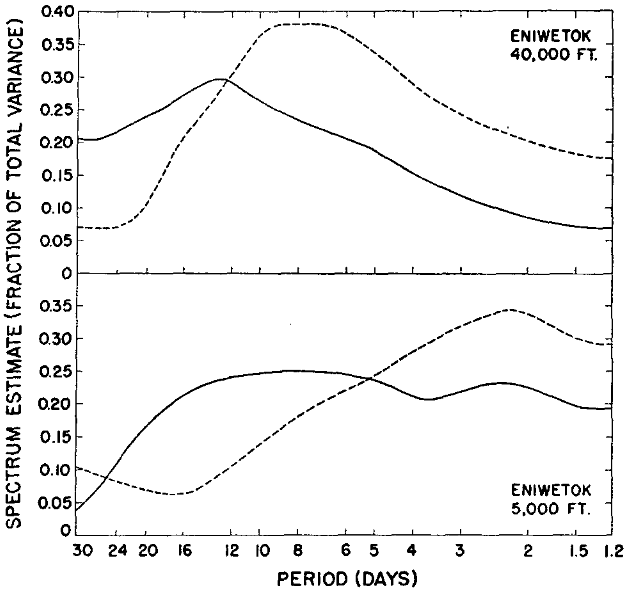

FIG. 4. Same as fig. 1 but for Eniwetok.

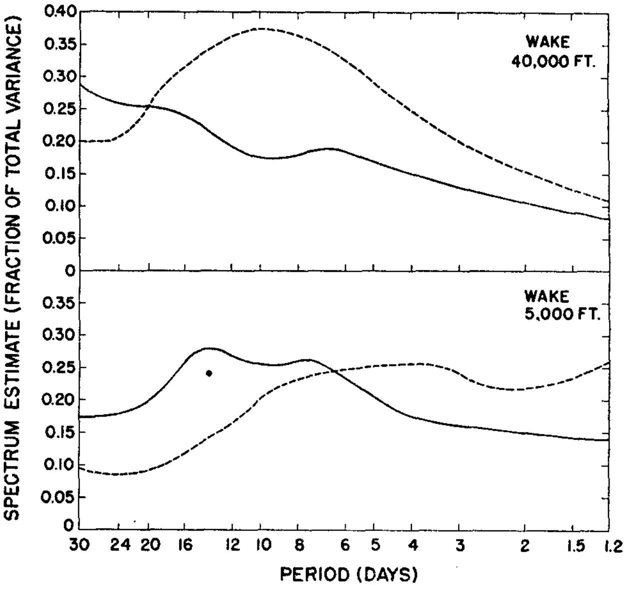

FIG. 6. Same as fig. 1 but for Wake.

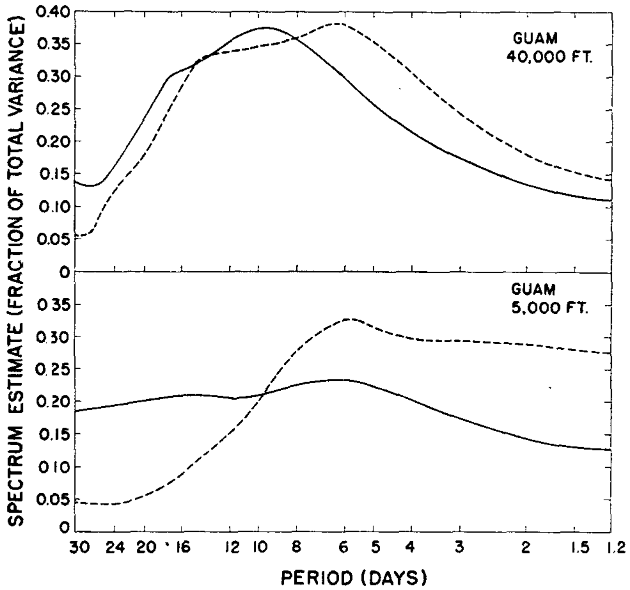

FIG. 5. Same as fig. 1 but for Guam.

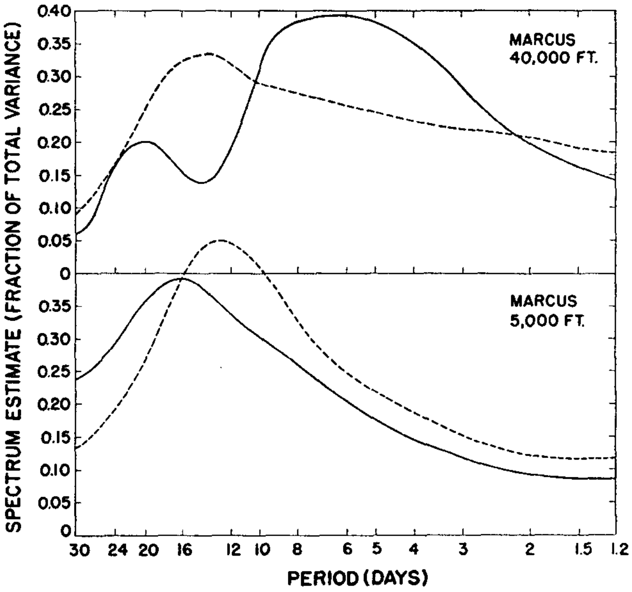

FIG. 7. Same as fig. 1 but for Marcus.

are somewhat strange. Here, meridional perturbation energy is almost equal for all periods less than 8 to 10 days and falls off to smaller values at the longer periods. At Marcus (fig. 7), which is the most northerly station considered here, but which is only some five degrees north of Wake, the $v$-spectrum is entirely different than that of the other stations. Here, a sharp maximum occurs close to 12 days; the spectrum falls off rapidly at longer periods and more gradually towards the shorter periods.

Turning our attention to the $u$-spectra at 5000 ft, we find they are, in most cases, markedly different than the corresponding $v$-spectra. In the $v$-spectra, relatively large amounts of energy were found at the shorter periods and relatively small amounts were found at the longer periods. In the $u$-spectra, the reverse situation appears to be the case. One exception to this is the $u$-spectrum at Eniwetok (fig. 4). At this station, almost equal partition of zonal-eddy energy is found for periods shorter than about 16 days, and the spectrum drops off rapidly at longer periods. The $u$-spectrum at Guam (fig. 5) is also somewhat different in appearance than those at the other stations. Here, there is very little difference in the proportion of eddy energy found in the various frequency bands. There is, however, some tendency for a maximum at a period of 6 days, and slightly smaller amounts of energy are found at the shorter periods.

At the other stations, the $u$-spectra generally show distinct maxima at periods in excess of 6 days. At Tarawa, Kapingamarangi, and Wake, these maxima are quite broad and cover a wide range of periods. At Tarawa, the primary maximum occurs between 6 and 8 days. The general area of maximum, however, extends from around 6 to 20 days. At Kapingamarangi, the maximum covers a range of periods of, roughly, from 8 to 20 days. At Wake, a broad maximum covers periods which range from 8 to about 14 or 15 days. At Marcus and Kusaie, however, the $u$-spectra show rather sharp maxima. At the former station, the maximum occurs close to 16 days and, at the latter station, close to 13 days.

*Forty-thousand feet.* With the exception of Marcus, all of the $v$-spectra show some sort of maximum within the range of periods of 5 to 10 days. It would seem that these maxima reflect the passage of the large-scale vortices which are so typical of the 40,000-ft level in these regions [4; 8] and which have been found by Riehl [8] to have a periodicity of about one week.

The $v$-spectra, generally, are shaped so that each has a single distinct maximum. Exceptions to this are Kusaie and Tarawa. At Kusaie, spectral values at periods below about 9 days are all very nearly equal, and smaller spectral values are found at periods in excess of 9 days. At Tarawa, the $v$-spectrum shows a secondary maximum near 20 days. Finally, it should be noted that the $v$-spectrum at Marcus has its maximum at a period of about 13 days. This is somewhat greater than the periods of spectral maxima at the other stations.

The $u$-spectra at 40,000 ft show a variety of shapes. At Guam and Eniwetok, there are single maxima which occur at periods of about 10 and 13 days, respectively. At Marcus, a strong maximum is found near 6 days with a secondary maximum occuring in the vicinity of 20 days. At Kapingamarangi, the primary maximum is found near 7 days, and a tendency for a secondary maximum near 30 days is also present. At Tarawa and Kusaie, the $u$-spectra have similar shapes. At these stations, the spectral curves rise with increasing period to a maximum, fall with further increasing period to a minimum, and finally begin to rise and continue to rise over the remainder of the range of periods considered. At Wake, the $u$-spectrum shows no distinct maximum but tends to rise with increasing period.

## 4. Conclusions

It seems fruitless to dwell upon the details of figs. 1 through 7 until their reality has been confirmed through examination of independent and more extensive data. We list below the conclusions that we feel can, with confidence, be drawn from the data examined here.

1. At 5000 ft, the $v$-spectra at Kapingamarangi and Tarawa show maxima at periods close to 4 days which are reflections of the passage of equatorial waves of the type described by Palmer [7].
2. In general, the $v$-spectra at 5000 ft show relatively large amounts of energy at shorter periods and relatively small amounts of energy at longer periods.
3. The $u$-spectra at 5000 ft generally show their maxima at periods in excess of 6 days.
4. The $v$-spectra at 40,000 ft, in general, show maxima at periods in the range of from 5 to 10 days. These maxima probably reflect the passage of large-scale upper vortices of the type described by Hubert [4] and Riehl [3; 8].
5. The normalized $v$-spectra (at both 5000 ft and 40,000 ft) tend to be greater than the normalized $u$-spectra for the shorter-period oscillations and less than the normalized $u$-spectra for the longer-period oscillations.

*Acknowledgment.* The author wishes to thank Mr. Donald Eilers for his assistance in "debugging" the IBM 704 program which was used to perform the computations reported on above.

## REFERENCES

1. Joint Task Force Seven, 1956: *Meteorological report on Operation Redwing, Part I, Meteorological Data* (12 Volumes).
2. Panofsky, H. A., and G. W. Brier, 1958: *Some applications of statistics to meteorology.* Univ. Park, Penn., Penn State Univ., 224 pp.
3. Riehl, H., 1954: *Tropical meteorology.* New York, McGraw-Hill, 392 pp.
4. Hubert, L. F., 1949: High tropospheric westerlies of the equatorial West Pacific Ocean. *J. Meteor.*, **6**, 216–224.
5. Kahn, A. B., 1957: A generalization of average-correlation methods of spectrum analysis. *J. Meteor.*, **14**, 9–17.
6. Estoque, M. A., 1955: The spectrum of large-scale turbulent transfer of momentum and heat. *Tellus*, **7**, 177–185.
7. Palmer, C. E., 1952: Tropical meteorology. *Quart. J. r. Meteor. Soc.*, **78**, 126–163.
8. Riehl, H., 1948: On the formation of typhoons. *J. Meteor.*, **5**, 247–264.